An industrial batch dryer simulation tool based on the concept of the characteristic drying curve

Kærn, Martin Ryhl; Elmegaard, Brian; Schneider, P.

Published in:
6th Nordic Drying Conference

Publication date:
2013

AN INDUSTRIAL BATCH DRYER SIMULATION TOOL BASED ON THE CONCEPT OF THE CHARACTERISTIC DRYING CURVE

M.R. Kærn[1], B. Elmegaard[1], P. Schneider[2]

[1]*Technical University of Denmark, Department of Mechanical Engineering,*
Nils Koppels Allé Bygn. 403, DK-2800 Lyngby, Denmark, email: pmak@mek.dtu.dk
[2]*Danish Technological Institute,*
Kongsvang Allé 29, DK-8000 Aarhus C, Denmark

Keywords: Industrial Batch Dryer, Characteristic Drying Curve, Modeling, Simulation

ABSTRACT

In this study an industrial batch dryer simulation tool is presented. The numerical model behind the scene is developed using the simulation software Engineering Equation Solver (EES) and compared to measurements from a batch dryer facility in Denmark producing insulation boards. In the constant-rate period, the model computes the average heat and mass transfer coefficients from EES built-in correlations for the actual flow configuration (rectangular duct flows). The transfer coefficients are used to compute the single stream heat and mass exchange effectiveness, assuming the temperature and moisture content in the material to be invariant in the airflow direction. In the falling-rate period, the concept of the Characteristic Drying Curve (CDC) is used as proposed by Langrish et al. (1991), but modified to account for a possible end-drying rate. Using the CDC both hygroscopic and non-hygroscopic materials may be analyzed by the tool and guidelines for the determination of the CDC coefficients are provided.

The comparison of the simulation tool with measurements shows that the assumption of invariant material properties along the flow direction is doubtful at least for the actual case of interest. However, the tool may be used to analyze overall effects of inlet temperature, volume flow rate, geometry, infiltration etc. on the performance in terms of drying time, heat consumption and blower power.

INTRODUCTION

The presented model is developed for general purpose industrial batch dryers and intended to be as simple as possible, yet able to capture the main effects of drying kinetics. The model is part of a larger simulation tool package called DryPack that may be used to design, dimension, analyze and optimize industrial drying processes. DryPack is mainly divided into 1) continuous dryer simulation and 2) batch dryer simulation. Whereas the current paper deals with a general batch dryer simulation model, a companion paper (Andreasen et al., 2013): "DryPack" – a calculation and analysis tool, describes the continuous dryer simulation models.

The batch dryer model is currently limited to convective drying processes, where hot humid air at atmospheric pressure flows across the product and supplies the latent heat of evaporation to the water inside the product. Other types of dryers such as indirect dryers (conduction heated) or radiation dryers are not supported currently.

For simplicity, the model of the product is assumed to be lumped. It means that the possible temperature and moisture content profiles are not resolved within the product. These profiles are important in the falling-rate period of drying, however, instead the concept of the Characteristic Drying Curve is used in the falling-rate period.

The concept of the Characteristic Drying Curve was first introduced by van Meel (1958) to a batch dryer. The concept has little (if any) theoretical foundation and is purely empirical. Keey (1978), Langrish (1999), Langrish and Kockel (2001), Langrish (2008) and co-workers have mostly (among others) explored the usefulness and evidence of the concept. Of materials studied by 14 authors, 12 materials obeyed the concept (Keey et al., 1985).

The concept postulates that for a wide range of drying conditions (temperature, humidity and flow rate) for a particular wet solid or product, the dimensionless characteristic drying curve becomes approximately the same. Its usage implies that 1) the critical moisture content is invariant and independent of initial moisture content, 2) the solid itself is geometrically similar, i.e. the exposed drying surface per unit volume is unchanged, and 3) the drying flow configuration is unchanged.

Other drying kinetic models include the receding evaporative interface and diffusion models, which need knowledge of the moisture diffusivity, thermal diffusivity and sorption data (if hygroscopic product). These models are based on specific mechanisms of drying as opposed to more empirical basis of the characteristic drying curve. Moreover, these models tend to ignore the complexity of the drying process where several transport mechanisms may operate simultaneously.

In the constant-rate period of drying the model computes the heat and mass transfer coefficients from EES own subroutines. However, the current version only supports the duct flow configuration. Since the product is assumed to be lumped at a single average temperature and moisture content, the surface temperature and water vapor mass fraction adjacent to the surface of the product is consequently lumped also. The effectiveness-NTU relations for single stream heat and mass exchangers are thus employed to compute the changes in temperature and mass fraction of the air across the dryer-oven. In turn the average water evaporation is found, together with the sensible and latent heat flows.

MODEL DESCRIPTION

A sketch of the batch dryer model is shown in Figure 1. The air flows as illustrated are quite general. The blower fan recirculates a specified volume flow through a heat input (heat exchanger) that delivers the heat according to the required inlet air temperature to the dryer-oven. The hot air

flows across the product and dries the product. To avoid hot water vapor leaving the dryer-oven to the surroundings, it is usually working at a slightly lower pressure, typically 500 Pa below atmospheric pressure. This causes air infiltration from the surroundings. The slightly lower pressure in the drying-oven is ensured by an air damper in the exhaust (not shown in Figure 1). The airflow through the exhaust is determined as a part of the recirculated air by using an exhaust parameter as

$$\dot{m}_{G,exhaust} = F \cdot \dot{m}_{G,blower} \tag{1}$$

where $\dot{m}_G$ is the mass flow rate of water vapor and dry air mixture.

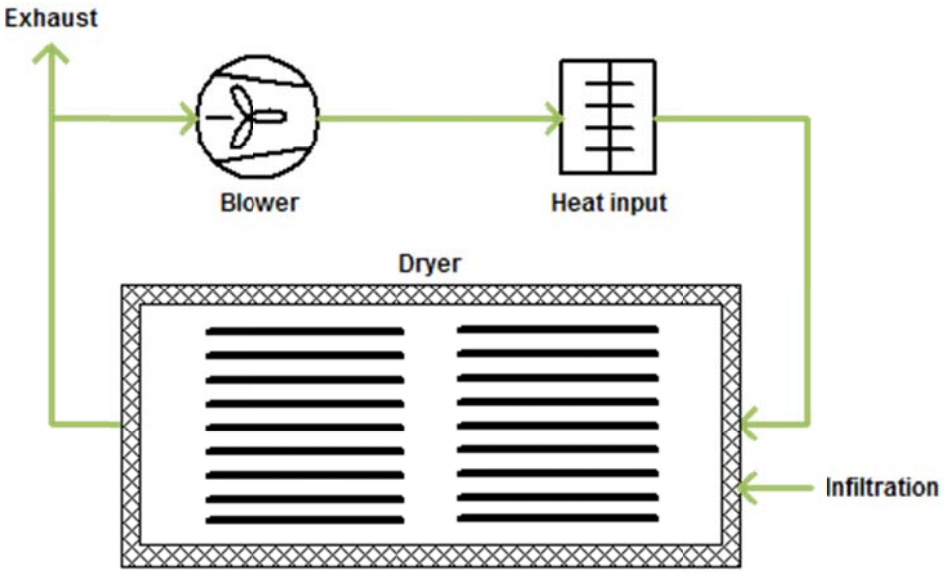

Figure 1. Sketch of batch dryer simulation tool

Integration

The model integrates the mass and energy conservation equations for the product as

$$M_S \frac{dX}{dt} = -\dot{m}_{evap} \tag{2}$$

$$M_S \frac{di_m}{dt} = -\dot{Q}_{cond} = -(\dot{Q}_{sens} + \dot{Q}_{lat}) \tag{3}$$

where the mean specific enthalpy of the product is defined as

$$i_m = \left(c_{p,S} + c_{p,W} \cdot X\right) T - \Delta h_s \cdot X \tag{4}$$

and Δh_s is the heat of desorption. The heat of desorption is only relevant for hygroscopic products, but is usually low compared to remaining terms (Keey, 1972; Mujumdar, 2007). For this reason Δh_s is neglected. Furthermore, the effects of sorption are assumed to be included in the actual characteristic drying curve.

The partial water vapor density of the air inside the dryer is integrated forward in time as

$$\frac{d\rho_v}{dt} = \frac{\dot{m}_{evap} + \dot{m}_{v,infil} - \dot{m}_{v,exhaust}}{V} \tag{5}$$

The initial conditions are thus temperature and moisture content of the product, whereas the initial partial water vapor density of the air inside the dryer is assumed to be that of the surroundings.
For simplicity, the energy conservation equation for the humid air inside the dryer-oven is assumed to be quasi-steady. The infiltration is assumed to happen evenly at the dryer inlet and outlet, respectively, thus resulting in a temperature and moisture content decrease of the airflow at these locations. The integration stops either at the specified stop time or when the required moisture content is reached.

Constant-rate period modeling

The constant drying rate period is not as complex as the falling-rate period. The theory for simultaneous heat and mass transfer is well established even for high mass transfer rate theory. In most drying conditions with air and water vapor mixture as the drying medium, usually low mass transfer rates occur, even at dry bulb temperatures from 100°C to 200°C. Also the wet bulb temperature may become as much as 80°C or more and still low mass transfer rates occur. The reason is because the difference in water vapor mass fraction between the mean air and the air adjacent to the solid surface is low even though these high temperatures occur. It means that the driving potential for mass transfer is relatively low. On the other hand this mass transfer is accomplished by the sensible heat transfer from the air to the solid/product. Only at extensive radiation or conductive (direct) heating may high mass transfer rates occur for drying with air/water vapor mixture at atmospheric pressure.
As mentioned previously, the effectiveness-NTU relations for single stream heat and mass exchangers are employed to compute the changes in temperature and mass fraction of the air across the dryer-oven, where the product (and surface) temperature and moisture content are assumed to be lumped, thus

$$\frac{m_{1,out} - m_{1,in}}{m_{1,s} - m_{1,in}} = 1 - e^{-g_{m1} \cdot A / \dot{m}_G} \tag{6}$$

$$\frac{T_{out} - T_{in}}{T_s - T_{in}} = 1 - e^{-h_c \cdot A / (\dot{m}_G \cdot c_p)} \tag{7}$$

Herein g_{m1} and h_c are the mass transfer conductance (often called the mass transfer coefficient) and heat transfer coefficient, respectively, as denoted by Mills (1999, 2001) and computed by EES built-in correlations for actual flow configuration (rectangular duct flows), using the heat and mass transfer analogy. Other correlations for other flow configurations may be adopted in future versions, thus not limiting the generality of the model. For a given mass flow of gas mixture, mass transfer conductance and heat transfer coefficient, the outlet mass fraction and temperature may be computed. The sensible and latent heat flows thus becomes

$$\dot{Q}_{sens} = \dot{m}_G \cdot c_p \cdot (T_{out} - T_{in}) \tag{8}$$

$$\dot{Q}_{lat} = \dot{m}_{evap} \cdot h_{fg} = \dot{m}_G (m_{1,out} - m_{1,in}) h_{fg} \tag{9}$$

Falling-rate period modeling

The use of the characteristic drying rate curve is essentially to model the falling-rate period by a non-dimensional empirical expression. The expression represents the actual drying rate at various temperatures, humidities and airflow rates. The characteristic drying curve is expressed as

$$\dot{m}'' = \dot{m}''_{CDR} \cdot f(\Phi) \tag{10}$$

Where $\dot{m}''$ is the actual drying rate (although it is a flux, i.e. per unit area), $\dot{m}''_{CDR}$ is the drying rate in the constant drying rate period and $f(\Phi)$ is a function of the dimensionless moisture content

$$\Phi = \frac{X - X^*}{X_c - X^*} \tag{11}$$

Many forms of $f(\Phi)$ has been proposed to fit typical solids. Langrish et al. (1991) presented a quite useful function that is used in the current model, but modified to include non-hygroscopic products also.

$$\begin{aligned} f(\Phi) &= f_F + (1 - f_F) \cdot \Phi^a && \Phi > \Phi_D \\ f(\Phi) &= f_F + (1 - f_F) \cdot \Phi_D^{a-b} \cdot \Phi^b && \Phi \le \Phi_D \end{aligned} \tag{12}$$

The modified function may fit all drying phases in the falling-rate period from point C-D-E (hygroscopic) or C-F (non-hygroscopic) in typical drying rate curves, see Figure 2.

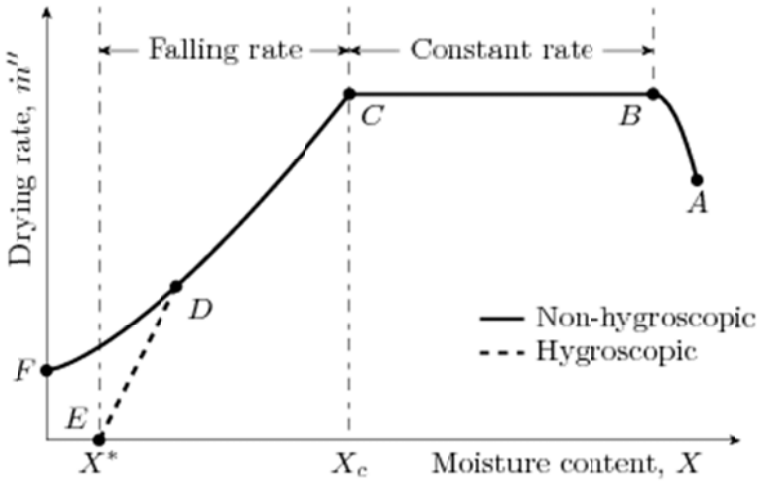

Figure 2. Typical drying curves, (Sattler and Feindt, 1995)

The possible characteristic drying curves using equation (12) are illustrated in Figure 3. The discontinuity at point D occurs only for hygroscopic products, thus for non-hygroscopic products $X^* = 0$, $\Phi_D = 0$ and exponent "b" becomes superfluous. Only the critical moisture content X_c, the end-drying rate f_F (terminal drying rate) and exponent "a" need be known for non-hygroscopic products, which may be viewed as similar to obtaining the liquid and vapor mass diffusivity and heat diffusivity in the product as functions of temperature and moisture content for rigorous

diffusion models. For hygroscopic products the sorption equilibrium data gives information on X^* and Φ_D (equilibrium moisture content and bound water limit, point D on Figure 2), and thus f_F, X_c, and exponents "a" and "b" need to be known.

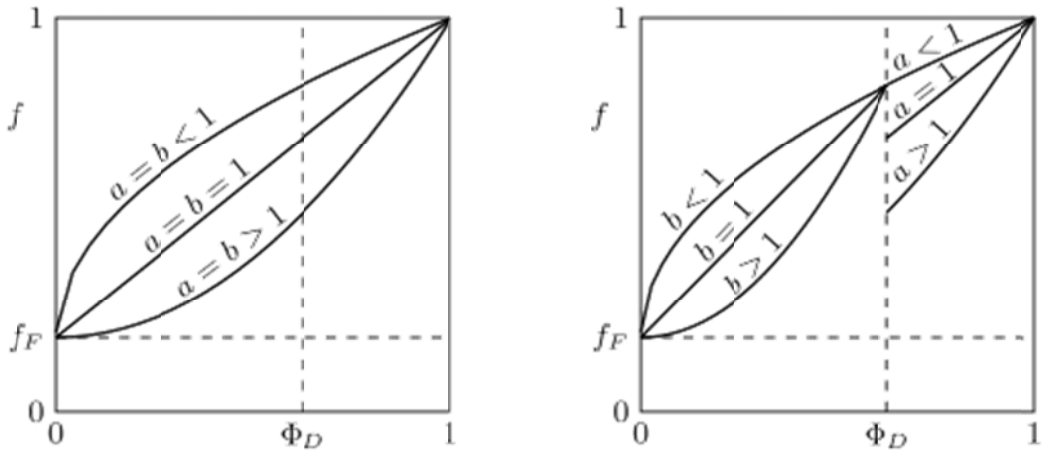

Figure 3. Possible characteristic drying curves using equation (12), (Mujumdar, 2007)

It should be stressed that the concept of the characteristic drying curve is to establish the coefficients above from small or pilot scale experiments, if not found from literature. These experiments may be carried out to give a set of characteristic drying curves at various initial moisture contents and at different exposed drying surface per unit volume. Such experiments may be performed by the authors. In addition, if large ranges of drying conditions are favored in terms of inlet temperature, humidity and airflow rate they must be parameterized also. As a first approximation, the help function in the simulation tool gives help for estimating approximate coefficients for various products.

Pressure drop and inlet temperature control

The model also computes the actual pressure loss through the rectangular duct system, again using EES built-in functions. Furthermore, we included the contraction and expansion losses according to Kays and London (1984), where the loss coefficients were fitted by graphical means. The rest of the piping system including the heat exchanger may be approximated by a system characteristic curve as depicted in Figure 4 using a nominal pressure drop and volume flow rate.

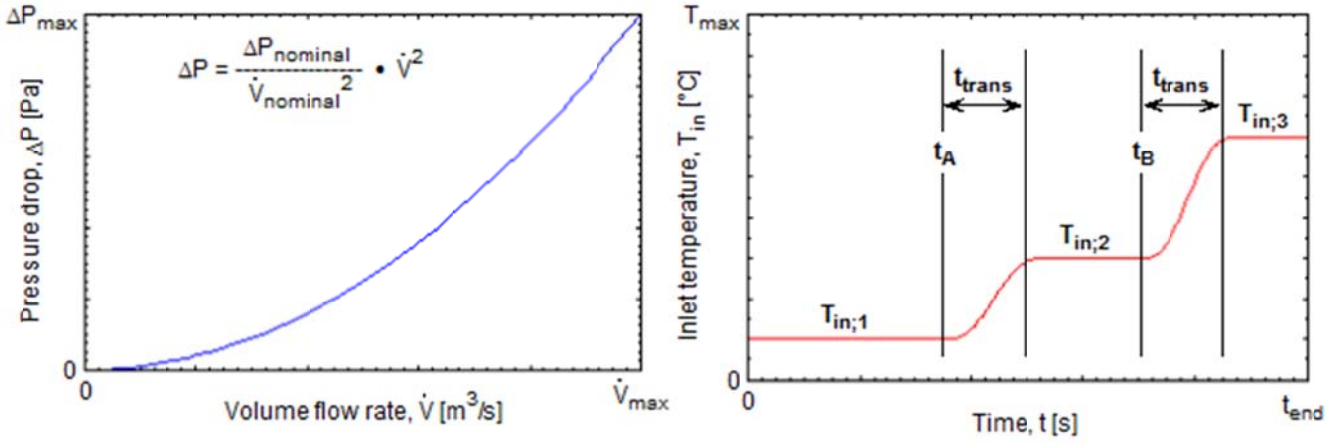

Figure 4. Auxiliary system characteristic curve (left) and Inlet temperature control (right)

In addition, it is possible to control the inlet temperature to the dryer oven at 3 different temperature stages in time and their transition time, which is modeled using a first order smooth transition function as given by Richter (2008).

EXPERIMENTAL COMPARISON AND RESULTS

The batch dryer model is compared against measurements from a Danish insulation board production facility. The insulation boards are placed on wagons with spacers in between and hot air flows through the small ducts between the spacers and dries the boards as illustrated on Figure 5. The wagons pass through two drying stages, a “pre-dryer” stage and a “post-dryer” stage, before reaching the required moisture content. In the current batch the inlet temperature were controlled to 160°C in both stages. There was, however, no information on the actual volume flow rates through the blower or the exhaust. In addition, there was little amount of knowledge to the characteristic drying curve. For these reasons the measurements may only serve as a comparison as opposed to a validation.

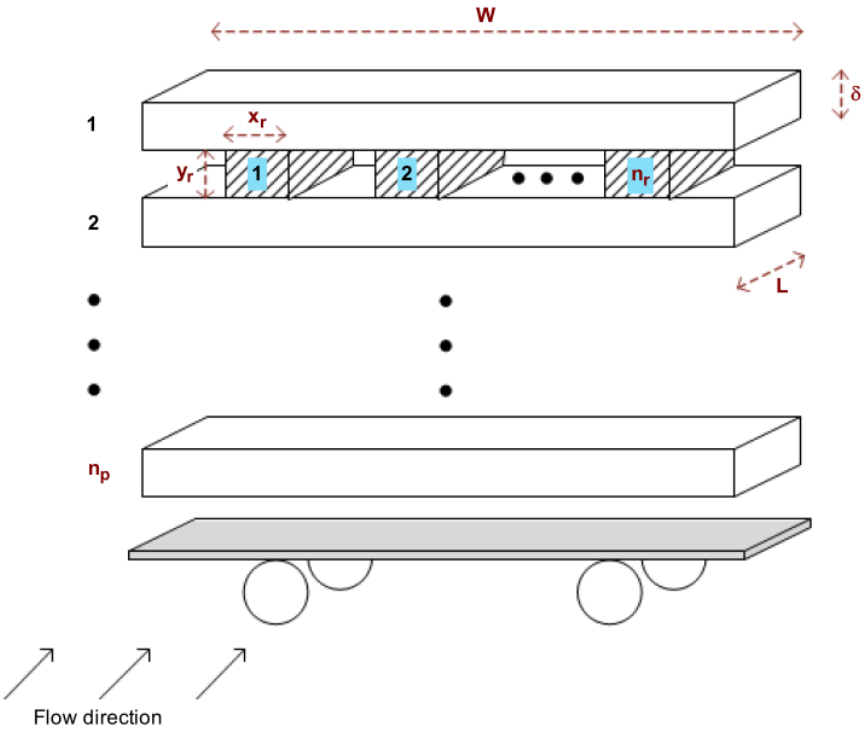

Figure 5. Flow configuration for drying of insulation boards

The inlet and outlet air temperatures to the dryer-oven were recorded together with the product surface temperature during a given batch. The total heat and mass transfer surface area was 665 m^2 and the product volume was 36.7m^3. The main bulk product is calcium silicate 50/50%. The porosity of the product was 0.91 % by volume and known to be non-hygroscopic. For non-hygroscopic materials, Keey (1972) recommended the exponent “a” to be 2 in equation 12, and hence used herein. The initial and final moisture content was 2.83 and 0.1 respectively, as given by the manufacturer.

We estimated the volume flow rate through the blower by integrating the energy rejected from the air in the measurements, which essentially must equal the energy needed to evaporate the water inside the product, thus

$$\dot{V} = \frac{M_W \cdot h_{fg}}{\int_{t_0}^{t_{end}} \rho \cdot c_p \cdot (T_{in} - T_{out})} \tag{13}$$

The result was 14 m^3/h. Additionally, we estimated an exhaust factor of 7% and used the product surface temperature measurement to adjust the critical moisture content to X_c=0.5 such that the constant-rate and falling-rate periods occur approximately at the same time. Moreover, the product surface temperature should be constant in the constant-rate period. In addition, we assumed a zero end-drying rate. The experimental comparison is shown on Figure 6 in terms of temperature development in time. Note again that the wagons pass thorough two similar drying stages, a "pre-dryer" and a "post-dryer". The superfluous and erroneous measurements in between the stages are omitted, and the simulation results are pushed forward in time accordantly.

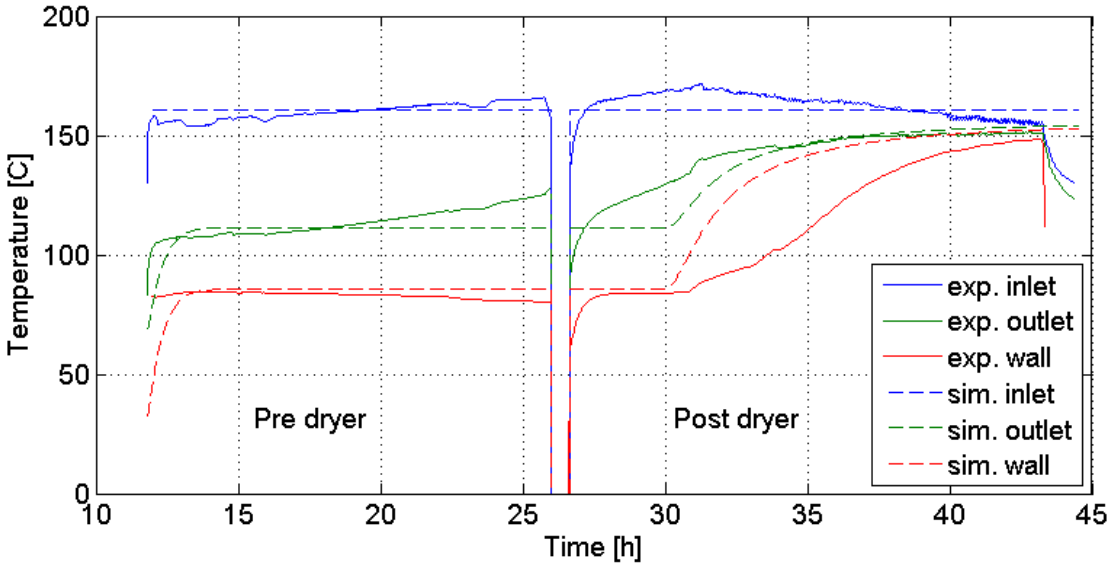

Figure 6. Experimental comparison of temperatures in the dryer oven

The experiments show clearly the constant-rate and falling-rate periods, i.e. the falling-rate period begins at approximately 31 hours. As expected the constant-rate and falling-rate periods are in accordance, due to the fitting of the critical moisture content. However, the outlet air temperature and surface temperature agree quite well and are reasonable predicted, at least in the constant-rate period, and when considering the model simplicity.

In the constant-rate period all air properties (temperatures, moisture contents) and surface properties become essentially constant in the model. It is also what we should expect from the model formulation. In contrast, the measurements show that the outlet temperature increases steadily during the constant-rate period. It is most likely due to a moisture gradient within the product along the flow direction, which is not accounted for in the current model. In other words, the upstream product dries quicker than the downstream product and reaches the critical moisture content sooner, thereby resulting in a steadily increasing outlet temperature. The current model assumes invariant material properties in the airflow direction. Nevertheless, the main temperature evolvement are captured and the simulation tool may be used to analyze important design and optimization parameters such as inlet temperature, volume flow rate and geometry layout in terms of drying time, heat consumption and blower power.

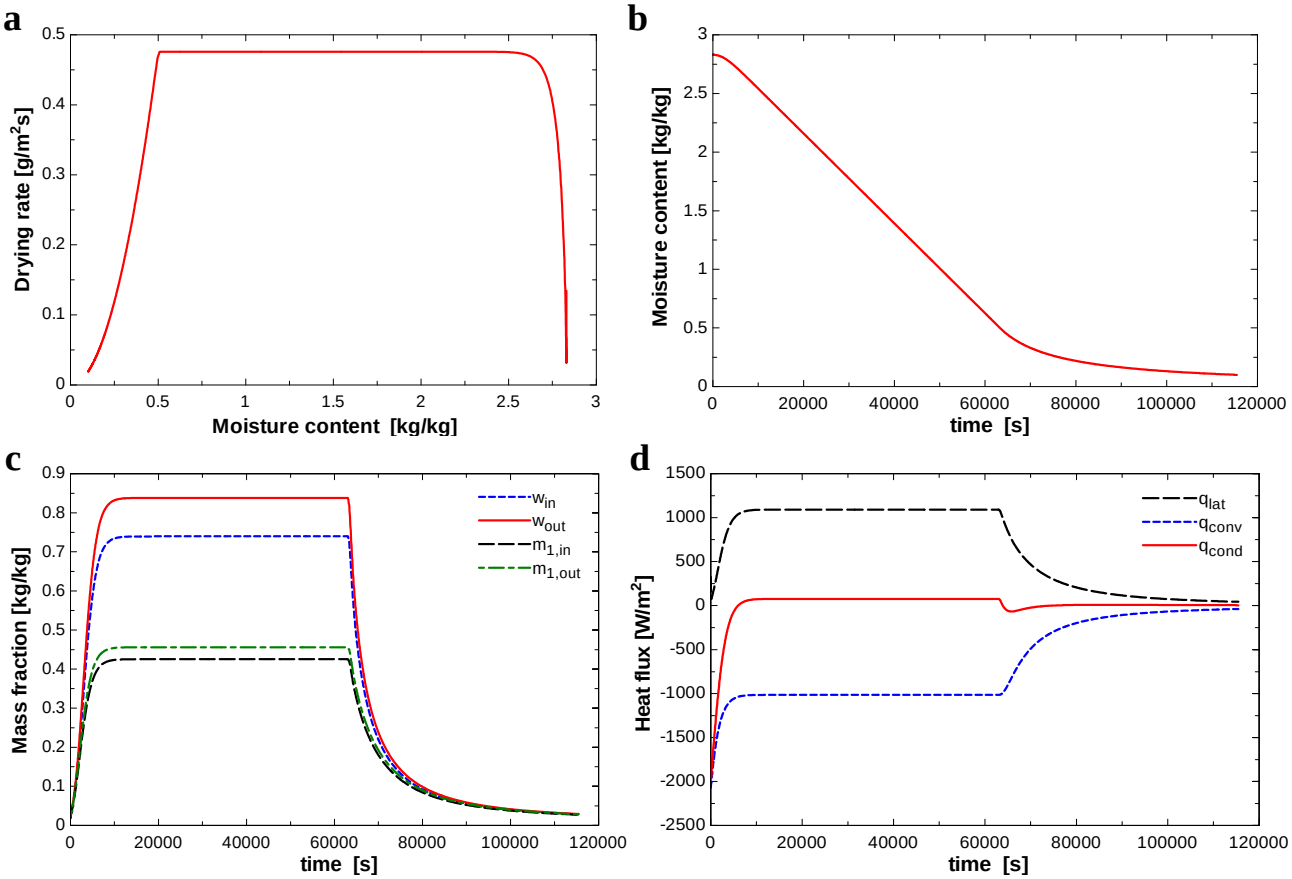

Figure 7. Additional model results from the experimental comparison

Figure 7 shows some of the available result plots in DryPack, which may be exported in .csv textural format. Figure 7a shows the actual drying rate curve that is a result of the constant-rate drying kinetics and the falling-rate characteristic drying rate curve. Figure 7b shows the drying rate as function of time, Figure 7c shows both humidity ratio and water vapor mass fraction as function of time and Figure 7d shows the heat fluxes to and from the product surface. All the figures show a clear distinction between the constant-rate and falling-rate periods.

CONCLUSIONS

A general model for an industrial batch dryer simulation tool called DryPack has been presented. The model is so far limited to duct flow configuration, but may easily be extended to other flow configurations, due to its born generality. The model is based on the concept of the Characteristic Drying Curve, and it is therefore important to supply a valid characteristic drying curve as input to the model that corresponds to the actual product and flow configuration. The tool gives help on estimating such input, however, it should be stressed that small or pilot scale experiments should be carried out to establish a valid characteristic drying rate curve. Such experiments may be carried out by the authors.

The model agrees well with experiments from a Danish insulation board production facility, when considering the simplicity of the model. The model may be used to analyze important design and optimization parameters such as inlet temperature, volume flow rate and geometry layout in terms of drying time, heat consumption and blower power.

NOTATION

Roman

A	Area	$[m^2]$
c_p	Specific heat capacity	[J/kg]
F	Exhaust factor	[-]
f	Dimensionless drying rate	[-]
f_F	Dimensionless end drying rate	[-]
g_{m1}	Mass transfer conductance	$[kg/m^2s]$
h_c	Convective heat transfer coefficient	$[W/m^2K]$
h_{fg}	Heat of evaporation	[J/kg]
i_m	Mean enthalpy of product	[J/kg]
M_S	Mass of dry bone solid product	[kg]
M_W	Mass of water in product	[kg]
m_1	Mass fraction of water vapor	[kg/kg]
$\dot{m}_G$	Mass flow rate of gas mixture	[kg/s]
P	Pressure	[Pa]
$\dot{Q}$	Heat flow rate	[W]
q	Heat flux	$[W/m^2]$
T	Temperature	[C]
t	Time	[s]
V	Volume	$[m^3]$
$\dot{V}$	Volume flow rate	$[m^3/s]$
w	Humidity ratio	[kg/kg]
X	Moisture content	[kg/kg]
X_c	Critical moisture content	[kg/kg]
X^*	Equilibrium moisture content	[kg/kg]

Greek

Δh_s	Heat of desorption	[J/kg]
ρ	Density	$[kg/m^3]$
Φ	Dimensionless moisture content	[-]

REFERENCES

Andreasen, M.B., Schneider, P., Kærn, M.R., Elmegaard, B., 2013. “DryPack” – a calculation and analysis tool. In: Sixth Nordic Drying Conference, Copenhagen, Denmark.

Kays, W.M., London, A.L., 1984. Compact heat exchangers. McGraw-Hill, New York, N.Y.

Keey, R.B., 1972. Drying. Principles and practice. Pergamon press, Oxford.

Keey, R.B., 1978. Introduction to industrial drying operations. Pergamon Press, Oxford.

Keey, R.B., Langrish, T.A.G., Reay, D., 1985. The applicability of the characteristic drying curve concept to the drying of porous particulate materials. In: Third Australasian Heat and Mass Transfer Conference. University of Melbourne, Victoria, Australia, pp. 102–110.

Keey, R.B., Suzuki, M., 1974. On the characteristic drying curve. International Journal of Heat and Mass Transfer 17 (12), 1455–1464.

Langrish, T.A.G., 1999. An assessment of the use of characteristic drying curves for the high-temperature drying of softwood timber. Drying Technology 17 (4-5), 991–998.

Langrish, T.A.G., 2008. Characteristic drying curves for cellulosic fibres. Chemical Engineering Journal 137 (3), 677–680.

Langrish, T.A.G., Bahu, R.E., Reay, D., 1991. Drying kinetics of particles from thin layer drying experiments. Chemical Engineering Research and Design 69 (5), 417–424.

Langrish, T.A.G., Kockel, T.K., 2001. The assessment of a characteristic drying curve for milk powder for use in computational fluid dynamics modelling. Chemical Engineering Journal 84 (1), 69–74.

Mills, A.F., 1999. Heat Transfer. Prentice Hall.

Mills, A.F., 2001. Mass Transfer. Prentice Hall.

Mujumdar, A.S., 2007. Handbook of industrial drying. CRC/Taylor & Francis, Boca Raton, FL.

Richter, C.C., 2008. Proposal of new object-oriented equation-based model libraries for thermodynamic systems. Ph.D. thesis, Technische Universität Carolo-Wilhelmina zu Braunschweig, Fakultät für Maschinenbau.

Sattler, K., Feindt, H.J., 1995. Thermal separation processes / Principles and design. Weinheim.

van Meel, D.A., 1958. Adiabatic convection batch drying with recirculation of air. Chemical Engineering Science 9 (1), 36–44.